

# Extrema of Two-Port Network Transducer Power Gain and Voltage Gain Under Varying Port Terminations: Semi-Analytical Method and Application to Biotelemetry System

Toni Björninen<sup>1</sup>

<sup>1</sup> BioMediTech Institute and Faculty of Biomedical Sciences and Engineering  
Tampere University of Technology, Tampere, 33101, Finland  
toni.bjorninen@tut.fi

**Abstract** — Analysis of the structure of the level sets of transducer power gain and voltage gain of a two-port network enables a semi-analytical method for finding the extrema these performance indicators as the port terminations vary in bounded rectangles in the complex plane. In particular, we show that the extrema are necessarily attained in small-dimensional subsets of the given rectangles. This provides efficient means to assess the impact of variability in the port terminations numerically. As an example, we study how variability in the port terminations affects the performance of a biotelemetry system composed of magnetically coupled small loops with highly sensitive impedance matching properties.

**Index Terms** — Two-port networks, tolerance analysis, sensitivity analysis, transducer power gain, voltage gain.

## I. INTRODUCTION

Fundamental optimisation approaches aim at maximising the performance of electromagnetic systems in their nominal operating conditions. In two-port microwave networks, which are the focus in this work, a typical goal is the bi-conjugate impedance matching that maximises the power transfer efficiency from the source to the load. This is a relevant goal in virtually all applications, including the recently emerged radio-frequency systems, which operate on harvested energy [1–4]. In such systems, however, also a certain voltage threshold must be exceeded to activate semiconductor devices. This makes the voltage gain another important parameter. A feature shared by both gain parameters in two-port systems is that they are non-linear functions of the complex impedances terminating the ports. Consequently, it is problematic to conclude how variability in the port terminations affect these fundamental performance indicators. In the related previous work, sensitivity of specific two-port networks was characterised through derivative-based approaches [5–6]. In article [7], the authors presented analysis of

constant mismatch circles to establish optimum trade-off between input and output mismatch for transistor amplifier design. The authors of [8] investigated the stability of two-port network with terminations varying in elliptic regions in the complex plane. In [4], the minimum of the voltage gain was computed numerically in a special case where the load impedance varied in a disk defined by a given lower bound of the transducer power gain.

In our earlier work [12], we showed that as the port terminations of a two-port network vary in bounded rectangles in the complex plane, the minimisers of the transducer power gain and voltage gain are located necessarily in small-dimensional subsets of the rectangles. In this work, we first summarise the relevant analytical considerations regarding the structure of the level sets of the gain parameters from [12] and then show how this enables identifying the subsets that necessarily contain the maximisers of the gain parameters. This way, we achieve the complete sensitivity analysis of two-port networks. The presented method does not involve differentiation, but is fully based on the analysis of the structure of the level sets of the gain parameters. It provides an efficient computation of the extrema of the gain parameters by restricting the search of both the minimum and maximum in small-dimensional subsets of the given tolerance rectangles. As an example, we apply the method in the analysis of a highly sensitivity biotelemetry system composed of magnetically coupled small loops.

## II. LEVEL SETS OF TRANSDUCER POWER GAIN AND VOLTAGE GAIN

Transducer power gain ( $G_t$ ) of a two-port network is the ratio of the power delivered to the load ( $Z_L=R_L+jX_L$ ) connected to Port 2 of the system to the power available from a Thévenin voltage source with internal impedance of  $Z_S=R_S+jX_S$  connected to Port 1. It is given by [1, Ch. 2]

$$G_i = \frac{4R_s R_L |z_{21}|^2}{|(Z_s + z_{11})(Z_L + z_{22}) - z_{12}z_{21}|^2}, \quad (1)$$

where  $z_{mn}$ , ( $m=1,2; n=1,2$ ) are the two-port Z-parameters. In this work, only passive port terminations and unconditionally stable systems are considered. In this case we have [1, Ch. 2]

$$\begin{cases} 0 < R_s \text{ and } 0 < R_L, \\ 0 < \text{Re}(z_{11}) \text{ and } 0 < \text{Re}(z_{22}), \\ |z_{12}z_{21}| < 2\text{Re}(z_{11})\text{Re}(z_{22}) - \text{Re}(z_{12}z_{21}), \end{cases} \quad (2)$$

which implies that the input and output impedances given by

$$Z_i = z_{11} - \frac{z_{12}z_{21}}{z_{22} + Z_L} \text{ and } Z_o = z_{22} - \frac{z_{12}z_{21}}{z_{11} + Z_s}, \quad (3)$$

respectively, have positive real parts.

The voltage gain ( $A_v$ ) of a two-port system is given by the ratio of the load (connected to Port 2) voltage amplitude to the amplitude of a Thévenin voltage source with internal impedance of  $Z_s = R_s + jX_s$  connected to Port 1. Basic circuit analysis utilising the Z-parameters yield

$$A_v = \frac{z_{21}Z_L}{(Z_s + z_{11})(Z_L + z_{22}) - z_{12}z_{21}}. \quad (4)$$

### A. Level sets of transducer power gain

For further analysis, it is useful to restate equation (1) as

$$\begin{cases} G_i = \frac{2\Lambda_L R_s}{|Z_s + Z_i|^2}, & \Lambda_L = \frac{2R_L |z_{21}|^2}{|Z_L + z_{22}|^2}, \\ G_o = \frac{2\Lambda_s R_L}{|Z_L + Z_o|^2}, & \Lambda_s = \frac{2R_s |z_{21}|^2}{|Z_s + z_{11}|^2}, \end{cases} \quad (5)$$

Next, we suppose that  $Z_s$  and Z-parameters are fixed and study the condition  $\alpha \leq G_i(Z_L)$ , where  $\alpha > 0$ . In this case, (5) implies

$$Z_L Z_L^* + \left(Z_o^* - \frac{\Lambda_s}{\alpha}\right) Z_L + \left(Z_o - \frac{\Lambda_s}{\alpha}\right) Z_L^* + |Z_o|^2 \leq 0, \quad (6)$$

which defines a complex plane disk  $D_{oL}$  with the centre point ( $C_{oL}$ ) and radius ( $r_{oL}$ ) given by

$$C_{oL} = -\left(Z_o^* - \frac{\Lambda_s}{\alpha}\right)^* = \frac{\Lambda_s}{\alpha} - Z_o \quad (7)$$

$$\text{and } r_{oL} = \sqrt{|C_{oL}|^2 - |Z_o|^2} = \sqrt{\frac{\Lambda_s}{\alpha} \left(\frac{\Lambda_s}{\alpha} - 2R_o\right)}.$$

Hence, for any  $Z_s$ , the load plane level set defined by  $\alpha = G_i(Z_L)$  is a circle and  $\alpha \leq G_i(Z_L)$  holds true in the disk  $D_{oL}$  bound by this circle. Analogously we find that for any  $Z_L$ , the source plane level set defined by  $\alpha = G_o(Z_s)$  is a circle with the centre point ( $C_{oS}$ ) and radius ( $r_{oS}$ ) given by

$$C_{oS} = \frac{\Lambda_L}{\alpha} - Z_i \text{ and } r_{oS} = \sqrt{\frac{\Lambda_L}{\alpha} \left(\frac{\Lambda_L}{\alpha} - 2R_i\right)}. \quad (8)$$

and that  $\alpha \leq G_o(Z_s)$  holds true in a disk  $D_{oS}$  bound by this circle.

By setting the radius to zero in equations (7)–(8), we find the level sets of  $G_i(Z_L)$  and  $G_o(Z_s)$  defined by  $\alpha = \Lambda_s/(2R_o)$  and  $\alpha = \Lambda_L/(2R_i)$  to be singletons  $\{C_{oL}\} = \{Z_o^*\}$  and  $\{C_{oS}\} = \{Z_i^*\}$ , respectively. These special cases correspond to complex-conjugate match at the output and input of the system, respectively, and for a larger  $\alpha$ , the level sets are empty. Thus, in the standard terminology of two-port systems,  $\Lambda_s/(2R_o) = G_a$  and  $\Lambda_L/(2R_i) = G_p$ , where  $G_a$  and  $G_p$  are the available power gain and operating power gain, respectively [1, Ch. 2]. Moreover, (7)–(8) show that the imaginary parts of  $C_{oL}$  and  $C_{oS}$  are independent of  $\alpha$ , whereas their real parts grow monotonically towards infinity as  $\alpha$  reduces. At the same time the radii  $r_{oL}$  and  $r_{oS}$  also tend monotonically towards infinity, but due to the level set property, for any  $\alpha_2 < \alpha_1$  we have  $D_{oS1} \subset D_{oS2}$  and  $D_{oL1} \subset D_{oL2}$ . Fig. 1 shows an illustration of the level sets of  $G_i$  in the source plane.

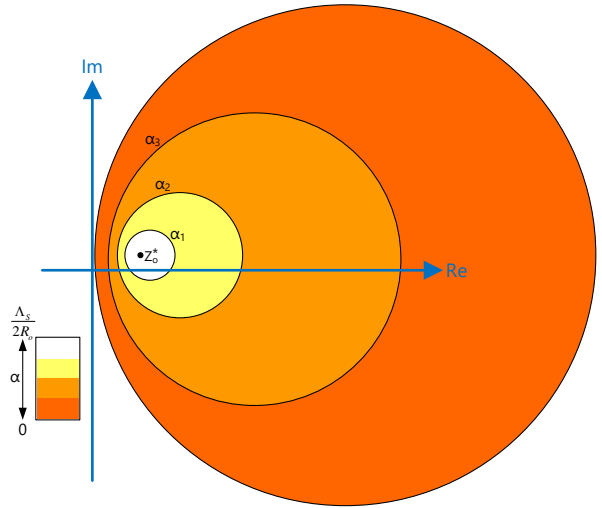


Fig 1. Illustration of the level sets of  $G_i$  in the load plane with  $\alpha_1 > \alpha_2 > \alpha_3$  [12].

### B. Level sets of voltage gain

First, we note that it is useful to restate equation (4) as

$$A_v = \Lambda \frac{Z_L}{|Z_L + Z_o|}, \quad \Lambda = \frac{z_{21}}{|Z_s + z_{11}|}. \quad (9)$$

Next, we suppose that  $Z_L$  and the Z-parameters are fixed and study the condition  $\alpha \leq A_v(Z_s)$ . In this case, (9) implies

$$|Z_s - C_{oS}| \leq \frac{1}{\alpha} \left| \frac{z_{21}Z_L}{Z_L + z_{22}} \right| = r_{oS}, \quad C_{oS} = -Z_i, \quad (10)$$

which defines a disk  $D_{as}$  with the centre point and radius of  $C_{as}$  and  $r_{as}$ , respectively. Hence, the level sets defined by  $\alpha = A_v(Z_S)$  are circles and  $\alpha \leq A_v(Z_S)$  holds true in  $D_{as}$ .

We suppose next that  $Z_S$  and the  $Z$ -parameters are fixed and study the condition  $\alpha \leq A_v(Z_L)$ . Now, (10) implies

$$Z_L Z_L^* + \frac{Z_o^*}{P} Z_L + \frac{Z_o}{P} Z_L^* + \frac{|Z_o|^2}{P} \begin{cases} \leq 0, & P > 0, \\ \geq 0, & P < 0, \end{cases} \quad (11)$$

where  $P = 1 - \Lambda^2/\alpha^2$ . For  $\alpha > \Lambda$ , (11) defines a complex plane disk  $D_{al}$  with the centre ( $C_{al}$ ) and radius ( $r_{al}$ ) given by

$$C_{al} = \frac{-Z_o}{P} \text{ and } r_{al} = \sqrt{|C_{al}|^2 - \frac{|Z_o|^2}{P}} = \frac{\Lambda}{\alpha} \left| \frac{Z_o}{P} \right|. \quad (12)$$

For  $\alpha < \Lambda$ , (11) defines the complex plane excluding  $D_{al}$ . Finally, in case  $\alpha = \Lambda$ , (11) defines a region comprised of the complex plane on and below the line

$$L_\Lambda = \left\{ x + jy : x = -\frac{X_o}{R_o} y - \frac{|Z_o|^2}{2R_o} \right\}. \quad (13)$$

Fig. 3 in Section IV illustrates of the level sets of  $A_v$  in the load plane. Finally, the limit processes for the level sets of  $A_v$  are summarised as follows:

$$\begin{aligned} \alpha \rightarrow 0 &\Rightarrow \begin{cases} r_{as} \rightarrow \infty \text{ and } C_{as} = -Z_i \\ r_{al} \rightarrow 0 \text{ and } C_{al} = 0 \end{cases} \\ \alpha \uparrow \Lambda &\Rightarrow \begin{cases} r_{al} \rightarrow \infty \\ C_{al} \rightarrow \infty \pm j\infty \\ D_{al} \rightarrow \text{Complex plane above } L_\Lambda \end{cases} \\ \alpha \downarrow \Lambda &\Rightarrow \begin{cases} r_{al} \rightarrow \infty \\ C_{al} \rightarrow -\infty \pm j\infty \\ D_{al} \rightarrow \text{Complex plane below } L_\Lambda \end{cases} \\ \alpha \rightarrow \infty &\Rightarrow \begin{cases} r_{as} \rightarrow 0 \text{ and } C_{as} \rightarrow -Z_i \\ r_{al} \rightarrow 0 \text{ and } C_{al} \rightarrow -Z_o \end{cases} \end{aligned} \quad (14)$$

### III. EXTREMA OF TRANSDUCER POWER GAIN

In this and the next section, we assume that the port terminations vary in a closed and bounded hyper-rectangle  $U = U_S \times U_L$  where  $U_S$  and  $U_L$  are rectangles in the complex plane given by

$$\begin{aligned} U_S &= \left\{ x + jy : 0 < x_{S1} \leq x \leq x_{S2}, \right. \\ &\quad \left. y_{S1} \leq y \leq y_{S2} \right\}, \\ U_L &= \left\{ x + jy : 0 < x_{L1} \leq x \leq x_{L2}, \right. \\ &\quad \left. y_{L1} \leq y \leq y_{L2} \right\}. \end{aligned} \quad (15)$$

Below, we will detail how the knowledge of the structure of the level sets of  $G_t$  and  $A_v$  enables the identification of small-dimensional subsets of  $U$  where the studied gain parameters necessarily attain their extreme values. To aid the further analysis, we denote the

sets of corner and boundary points of  $U_S$  and  $U_L$  by  $V_S$  and  $V_L$ , and  $B_S$  and  $B_L$ , respectively.

Since  $G_t$  and  $A_v$  are continuous real-valued functions which can also be interpreted as functions of four real variables in a closed and bounded set defined by the intervals of the real and imaginary parts in equation (15), Extreme Value Theorem guarantees that they attain their extreme values in  $U$  [9, Ch. 12.5].

#### B. Minimum of transducer power gain

The level sets of  $G_t$  are circles in both the source and load planes. We focus first on the source plane, where  $\alpha \leq G_t(Z_S)$  holds true in a disk  $D_{as}$  which is bound by the level set circle. Hence, to bound  $G_t(Z_S)$  from below in  $U_S$ , we must find the smallest  $\alpha$  for which  $U_S$  is entirely contained in  $D_{as}$ . Since  $U_S$  is a rectangle, such  $\alpha$  defines a level set circle that passes through a corner of  $U_S$ . Hence, for all  $Z_S$  in  $U_S$  we have  $G_t(Z_S) \geq G_t(Z_{S0})$ , where  $Z_{S0} \in V_S$ . With a similar reasoning, for all  $Z_L$  in  $U_L$ , we have  $G_t(Z_L) \geq G_t(Z_{L0})$ , where  $Z_{L0} \in V_L$ . Consequently, for all  $(Z_S, Z_L)$  in  $U$ :  $G_t(Z_S, Z_L) \geq G_t(Z_{S0}, Z_L) \geq G_t(Z_{S0}, Z_{L0})$ . Because this lower bound of  $G_t$  over the whole closed and bounded set  $U$  is its value evaluated at  $(Z_{S0}, Z_{L0}) \in U$ , then by the Extreme Value Theorem, this point must be the minimiser of  $G_t$  in  $U$ .

#### C. Maximum of transducer power gain

For an unconditionally stable two-port, the unique bi-conjugate-matched source and load terminations  $Z_{mS}$  and  $Z_{mL}$ , respectively, maximise the transducer power gain and the maximum can be computed with the well-known formula [1, Ch. 2]. Clearly, if  $(Z_{mS}, Z_{mL}) \in U$ , this point is the maximiser of  $G_t$  in  $U$ . Therefore, below we will assume that  $(Z_{mS}, Z_{mL}) \notin U$ . For further analysis, we denote the images of  $U_L$  and  $U_S$  under the complex conjugate map of the input and output impedances as  $Z_i^*[U_L]$  and  $Z_o^*[U_S]$ , respectively, and make the following definitions:  $\Sigma_S = U_S \cap Z_i^*[U_L]$  and  $\Sigma_L = U_L \cap Z_o^*[U_S]$ .

If  $\Sigma_S$  and  $\Sigma_L$  are both empty, then for an increasing level sets values, the level set circles of  $G_t$  must converge towards points outside of  $U_S$  and  $U_L$ , because neither the input or output can be conjugate-matched. Hence, to bound  $G_t(Z_S, Z_S)$  from above in  $U_S$ , we must find the largest level set value  $\alpha$  for which  $D_{as}$  intersects  $U_S$  at a single point only. Such  $\alpha$  defines a level set circle that passes through a point in the boundary of  $U_S$ . Hence, for all  $Z_L$  in  $U_L$ , we have  $G_t(Z_S, Z_L) \leq G_t(Z_{S0}, Z_L)$ , where  $Z_{S0} \in B_S$ . With an identical argument, for any  $Z_S \in U_S$ , we have  $G_t(Z_S, Z_L) \leq G_t(Z_S, Z_{L0})$ , where  $Z_{L0} \in B_L$ . Consequently, for all  $(Z_S, Z_L)$  in  $U$ :  $G_t(Z_S, Z_L) \leq G_t(Z_{S0}, Z_L) \leq G_t(Z_{S0}, Z_{L0})$ . Because this upper bound of  $G_t$  over the whole closed and bounded set  $U$  is its value evaluated at  $(Z_{S0}, Z_{L0}) \in U$ , by the Extreme Value Theorem, this point must be the maximiser of  $G_t$  in  $U$ .

If either  $\Sigma_S$  or  $\Sigma_L$  or both are non-empty, the maximiser of  $G_t$  may be located in the interior of  $U$ . To

aid the analysis in these cases, we first study the algebraic properties of the map  $Z_i^*$  defined as the

complex conjugate of the input impedance. Firstly,  $Z_i^*$  is clearly continuous in  $U_L$  since  $\text{Re}(z_{22})$  and  $R_L$  are both positive (equation 2) and thus  $z_{22} + Z_L \neq 0$  in equation (3). Moreover, it is elementary to show that  $Z_i^*$  is injective and thus bijective from its domain to its image. Finally, equation (3) can be readily solved for  $Z_L$  to see that the inverse map  $Z_i^{*-1}$  exists and is continuous. These properties make  $Z_i^*$  a homeomorphism from  $U_L$  to its image. This class of functions map interior and boundary points of their domain to the respective points of the image. Moreover, simply-connectedness is a property that is preserved under a homeomorphic map. Therefore, as the closed and bounded rectangle  $U_L$  is clearly simply-connected, so must be the set  $Z_i^*[U_L]$ .

With analogous arguments as for the map  $Z_i^*$ , we find that  $Z_i^{*-1}$  is a homeomorphism from  $\Sigma_S$  to its image  $Z_i^{*-1}[\Sigma_S]$  and thus this set must be simply-connected and its boundary given by  $Z_i^{*-1}[\partial\Sigma_S]$ , where  $\partial\Sigma_S$  denotes the boundary of  $\Sigma_S$ . Since  $Z_i^*$  and  $Z_o^*$  have identical structure, all of the above conclusions are true for  $Z_o^*$  and its inverse as well. Finally, we note that since we have assumed that the bi-conjugate-matched source and load impedances of the two-port system are not located in  $U$ , we must have  $\Sigma_S \cap Z_o^{*-1}[\Sigma_L] = \emptyset$  and  $\Sigma_L \cap Z_i^{*-1}[\Sigma_S] = \emptyset$ .

Next, we suppose  $\Sigma_S$  is non-empty. This implies that there exists  $Z_{L1} \in Z_i^{*-1}[\Sigma_S]$  such that  $Z_i^*(Z_{L1}) = Z_{S1} \in \Sigma_S$ . In general,  $G_t(Z_S, Z_L) \leq G_p(Z_L)$ , where  $G_p$  is the operating power gain of the two-port network attained when the input is conjugate-matched. Because the input is conjugate-matched at the point  $(Z_{S1}, Z_{L1})$ ,  $G_t$  attains its upper bound  $G_p(Z_L)$  w.r.t. the source impedance at this point. However, since  $\Sigma_L \cap Z_i^{*-1}[\Sigma_S] = \emptyset$ , the level sets of  $G_t$  in the load plane converge towards a point outside of  $Z_i^{*-1}[\Sigma_S]$ . Hence, to bound  $G_t$  from above in  $\Sigma_S \times Z_i^{*-1}[\Sigma_S]$ , we must find the largest  $\alpha$  for which  $D_{\alpha L}$  intersects  $Z_i^{*-1}[\Sigma_S]$  at a single point only. Such  $\alpha$  defines a level set circle that passes through a point in the boundary of  $Z_i^{*-1}[\Sigma_S]$ . Thus, for all  $(Z_S, Z_L) \in \Sigma_S \times Z_i^{*-1}[\Sigma_S]$ , we have  $G_t(Z_S, Z_L) \leq G_t(Z_{S1}, Z_{L1})$ , where  $Z_{L1} \in Z_i^{*-1}[\partial\Sigma_S]$  and  $Z_{S1} = Z_i^*(Z_{L1})$ .

In case  $\Sigma_L$  is non-empty, then by identical arguments as above, we have  $G_t(Z_S, Z_L) \leq G_a(Z_S)$ , where  $G_a$  is the available power gain of the two-port network attained when the output is conjugate-matched and we conclude that for all  $(Z_S, Z_L) \in Z_o^{*-1}[\Sigma_L] \times \Sigma_L$  we have  $G_t(Z_S, Z_L) \leq G_t(Z_{S2}, Z_{L2})$ , where  $Z_{S2} \in Z_o^{*-1}[\partial\Sigma_L]$ ,  $Z_{L2} = Z_o^*(Z_{S2})$ . Finally, since  $\Sigma_S \times Z_i^{*-1}[\Sigma_S]$  and  $\Sigma_L \times Z_o^{*-1}[\Sigma_L]$  are proper subsets of  $U$ , the upper bound of  $G_t$  in the whole  $U$  may be larger than  $\max\{G_t(Z_{S1}, Z_{L1}), G_t(Z_{S2}, Z_{L2})\}$ . However, for a level set value  $\alpha$  that is strictly greater than this value, the level sets of  $G_t$  are either empty, if  $(Z_{S1}, Z_{L1})$  or  $(Z_{S2}, Z_{L2})$  happens to be the maximiser of  $G_t$  in  $U$ , or converge towards points outside of  $U_S$  and  $U_L$ .

This is because, in all cases where level sets convergence towards a point inside  $U_S$  or  $U_L$ ,  $G_t$  is upper bounded by  $\max\{G_t(Z_{S1}, Z_{L1}), G_t(Z_{S2}, Z_{L2})\} < \alpha$  as shown above. Thus, for all  $(Z_S, Z_L) \in U$ , we have  $G_t(Z_S, Z_L) \leq \max\{G_t(Z_{S0}, Z_{L0}), G_t(Z_{S1}, Z_{L1}), G_t(Z_{S2}, Z_{L2})\}$ , where  $(Z_{S0}, Z_{L0}) \in B_S \times B_L$ .

Based on these findings, we conclude that the maximiser of  $G_t$  in  $U$  is necessarily located in a small-dimensional subset of  $U$  as summarised below. Fig. 2 illustrates the search of the maximiser of  $G_t$  in  $U_L$  in case (d) of the below list.

- (a) If  $(Z_{mS}, Z_{mL}) \in U$ , the maximum of  $G_t$  in  $U$  is  $G_t(Z_{mS}, Z_{mL})$ .
- (b) If  $\Sigma_S = \emptyset$  and  $\Sigma_L = \emptyset$ , the maximiser of  $G_t$  in  $U$  is a point  $(Z_{S0}, Z_{L0}) \in B_S \times B_L$ .
- (c) If  $\Sigma_S \neq \emptyset$  and  $\Sigma_L = \emptyset$ , the maximiser of  $G_t$  in  $U$  is  $(Z_{S0}, Z_{L0})$  or a point  $(Z_{S1}, Z_{L1})$ , where  $Z_{L1} \in Z_i^{*-1}[\partial\Sigma_S]$  and  $Z_{S1} = Z_i^*(Z_{L1})$ .
- (d) If  $\Sigma_S = \emptyset$  and  $\Sigma_L \neq \emptyset$ , the maximiser of  $G_t$  in  $U$  is  $(Z_{S0}, Z_{L0})$  or a point  $(Z_{S2}, Z_{L2})$ , where  $Z_{S2} \in Z_o^{*-1}[\partial\Sigma_L]$  and  $Z_{L2} = Z_o^*(Z_{S2})$ .
- (e) If  $\Sigma_S \neq \emptyset$  and  $\Sigma \neq \emptyset$ , the maximiser of  $G_t$  in  $U$  is  $(Z_{S0}, Z_{L0})$ ,  $(Z_{S1}, Z_{L1})$  or  $(Z_{S2}, Z_{L2})$ .

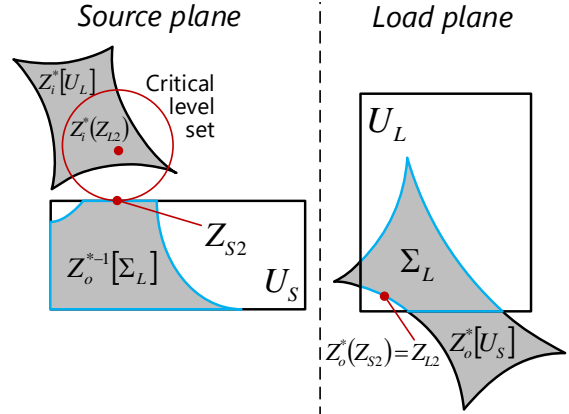


Fig 2. Illustration of the search of maximiser of  $G_t$  in  $U$  in the case  $\Sigma_S = \emptyset$  and  $\Sigma_L \neq \emptyset$ . The figure has been drawn supposing the maximiser is  $(Z_{S2}, Z_{L2})$ .

## IV. EXTREMA OF VOLTAGE GAIN

### A. Minimum of voltage gain

In the source plane, the level sets defined by  $\alpha = A_v(Z_S)$  are circles given in equation (9) and  $\alpha \leq A_v(Z_S)$  holds true in a disk  $D_{\alpha S}$  which is bound by the level set circle. Hence, to bound  $A_v(Z_S)$  from below in  $U_S$ , we must find the smallest  $\alpha$  for which  $U_S$  is contained in  $D_{\alpha S}$ . Since  $U_S$  is a rectangle, such  $\alpha$  defines a level set circle which passes through a corner of  $U_S$ . As seen from equation (9), the centre point of the level set circle has a negative real part and the circle radius is inversely proportional to  $\alpha$ . Therefore, since every point in  $U_S$  has a positive real part,

the set of possible corners of intersection are limited to those with larger real parts. We denote these corners as  $V_{S+} = \{x_{S2} + jy_{S1}, x_{S2} + jy_{S2}\}$ . Hence, for all  $Z_S$  in  $U_S$  we have  $A_v(Z_S) \geq A_v(Z_{S0})$ , where  $Z_{S0} \in V_{S+}$ .

To bound  $A_v(Z_L)$  from below in  $U_L$ , we first suppose that the minimum of  $A_v(Z_L)$  in  $V_L$  is attained at a point  $Z_{L1}$ . If  $A_v(Z_{L1}) > \Lambda$ , then the level set circle that passes through  $Z_{L1}$  must be the boundary of a disk  $D_{al}$  where  $A_v(Z_L) \geq A_v(Z_{L1})$ . Given that  $Z_{L1}$  is a corner point of  $U_L$  and minimises  $A_v(Z_L)$  in  $V_L$ , then the remaining corners of  $U_L$  must be contained in  $D_{al}$ . Since  $U_L$  is a rectangle, this implies that  $U_L$  must be entirely contained  $D_{al}$ . Thus,  $A_v(Z_L) \geq A_v(Z_{L1})$  for all  $Z_L$  in  $U_L$ .

If  $A_v(Z_{L1}) < \Lambda$ , there may be more points in  $U_L$  for which  $A_v$  is smaller than  $A_v(Z_{L1})$ . For any such point  $Z_{L2}$ ,  $A_v(Z_L) \geq A_v(Z_{L2})$  holds true outside of  $D_{al}$  with the corresponding level set circle passing through  $Z_{L2}$ . Thus, to bound  $A_v(Z_L)$  from below in  $U_L$ , we must find the smallest  $\alpha$  such that  $D_{al}$  intersects  $U_L$  at a single point only. Based on the limit processes summarised in equation (14), as  $\alpha$  reduces from  $\Lambda$  towards 0, then  $C_{al} \rightarrow 0$  and  $r_{al} \rightarrow 0$ . However, by the definition of  $U_L$  given in equation (15),  $0 \notin U_L$ . Thus, the intersection point must be found in  $B_L$ .

By combining the results from the above discussion, since  $V_L \subset B_L$ , for all  $(Z_S, Z_L)$  in  $U$  we have  $A_v(Z_S, Z_L) \geq A_v(Z_{S0}, Z_L) \geq A_v(Z_{S0}, Z_{L0})$ , where  $(Z_{S0}, Z_{L0}) \in V_{S+} \times B_L$ . Because this lower bound of  $A_v$  over the whole closed and bounded set  $U$  is its value evaluated at  $(Z_{S0}, Z_{L0}) \in U$ , then by the Extreme Value Theorem, this point must be the minimiser of  $A_v$  in  $U$ . Figure 3 illustrates the search of the minimiser of  $A_v$  in  $U_L$ .

## B. Maximum of voltage gain

In the source plane, the level sets defined by  $\alpha = A_v(Z_S)$  are circles given in equation (9) and  $\alpha \leq A_v(Z_S)$  holds true in a disk  $D_{as}$  which is bound by the level set circle. Hence, to bound  $A_v(Z_S)$  from above in  $U_S$ , we must find the largest  $\alpha$  for which  $D_{as}$  intersects  $U_S$  only at a single point. Since  $U_S$  is a rectangle, such  $\alpha$  defines a level set circle that passes through a point at the boundary of  $U_S$ . As seen from equation (9), the centre point of the level set circle has a negative real part and the circle radius is inversely proportional to  $\alpha$ . Therefore, since every point in  $U_S$  has a positive real part, the intersection point must lie on the vertical edge of  $U_S$  with the smaller real part. We denote this set as  $B_{S-} = \{x + jy: x = x_{S1}, y_{S1} \leq y \leq y_{S2}\}$ . Hence, for all  $Z_S$  in  $U_S$  we have  $A_v(Z_S) \leq A_v(Z_{S0})$ , where  $Z_{S0} \in B_{S-}$ .

To bound  $A_v(Z_L)$  from above in  $U_L$ , we first suppose that the maximum of  $A_v(Z_L)$  in  $V_L$  is attained at a point  $Z_{L1}$ . If  $A_v(Z_{L1}) < \Lambda$ , the level set circle passing through  $Z_{L1}$  defines a disk  $D_{al}$  where  $A_v(Z_L) < A_v(Z_{L1})$ . Given that  $Z_{L1}$  is a corner point of  $U_L$  and maximises  $A_v(Z_L)$  in  $V_L$ , the remaining corners must be contained in  $D_{al}$ . Since  $U_L$  is

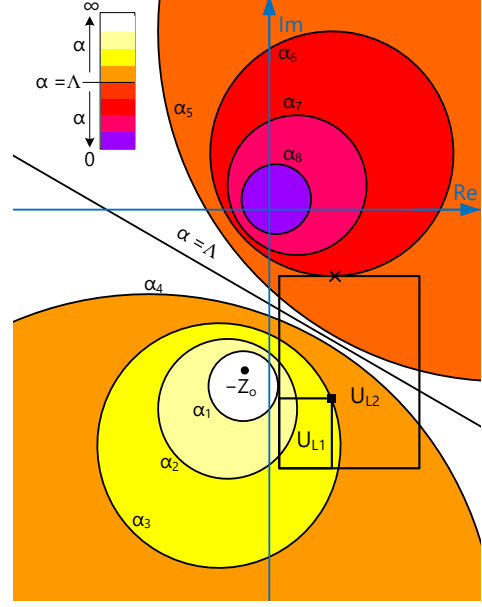


Fig. 3. Illustration of the search of minimiser of  $A_v$  in the load plane in rectangles  $U_{L1}$  and  $U_{L2}$ . In the figure:  $\alpha_n > \alpha_{n+1}$  and  $\alpha_4 > \Lambda > \alpha_5$ . The box and cross markers indicate the minimiser of  $A_v$  in  $U_{L1}$  and  $U_{L2}$ , respectively [12].

a rectangle, this implies that  $U_L$  must be entirely contained in  $D_{al}$ . Thus,  $A_v(Z_L) < A_v(Z_{L1})$  for all  $Z_L$  in  $U_L$ .

If  $A_v(Z_{L1}) > \Lambda$ , there may be more points in  $U_L$  for which  $A_v$  is greater than  $A_v(Z_{L1})$ . For any such point  $Z_{L2}$ ,  $A_v(Z_L) \leq A_v(Z_{L2})$  holds true outside of  $D_{al}$  with the corresponding level set circle passing through  $Z_{L2}$ . Thus, to bound  $A_v(Z_L)$  from above in  $U_L$ , we must find the largest  $\alpha$  such that  $D_{al}$  intersects  $U_L$  at a single point only. Based on the limit processes summarised in equation (14), as  $\alpha$  grows from  $\Lambda$  towards infinity,  $C_{al} \rightarrow 0$  and  $r_{al} \rightarrow 0$ . By the definition of  $U_L$  given in equation (15),  $0 \notin U_L$ . Thus, the intersection point must be found in  $B_L$ .

By combining the results from the above discussion, since  $V_L \subset B_L$ , for all  $(Z_S, Z_L)$  in  $U$  we have  $A_v(Z_S, Z_L) \leq A_v(Z_{S0}, Z_L) \leq A_v(Z_{S0}, Z_{L0})$ , where  $(Z_{S0}, Z_{L0}) \in B_{S-} \times B_L$ . Because this upper bound of  $A_v$  over the whole closed and bounded set  $U$  is its value evaluated at  $(Z_{S0}, Z_{L0}) \in U$ , then by the Extreme Value Theorem, this point must be the minimiser of  $A_v$  in  $U$ .

In practice, the search for the maximiser of  $A_v$  in  $U$  is initialised by finding the maximiser  $(Z_{S0}, Z_{L1})$  of  $A_v$  in  $B_{S-} \times V_L$ . This is readily done, since this is a small subset of  $U$ . Next  $\Lambda$  given in equation (9) is computed at  $Z_S = Z_{S0}$ . If  $A_v(Z_{S0}, Z_{L1}) < \Lambda$ , then  $(Z_{S0}, Z_{L1})$  maximises  $A_v$  in  $U$ . Otherwise, the maximum value is attained in  $B_{S+} \times B_L$  which is also a limited subset of  $U$ . The search for the minimiser follows an analogous algorithm.

## V. APPLICATION TO ANALYSIS OF A BIOTELEMETRY SYSTEM

The presented technique of finding the extrema of the transducer power gain and voltage gain of a two-port network as the source and load impedances vary in given rectangles in the complex plane is applicable to all two-ports which are unconditionally stable. In this section, we present an example in the analysis of a wireless link in a biotelemetry system.

We consider a wireless link between a miniature loop antenna formed by metallizing four adjacent faces of a  $1 \times 1 \times 1$  mm<sup>3</sup> sized cube and a planar circular loop with the inner diameter of 12 mm, which has been developed for a wireless brain-machine interface system [3]. In this application, the cubic loop lies on the cortex harvesting energy for a microsystem that records the electrical activity of the brain. The source of energy is a planar loop placed 5 mm above the scalp transmitting at 300 MHz. A major practical challenge in the implementation and testing of the wireless link is the impedance matching of the small loops. This is because they have very low input resistance and consequently the system is sensitive towards variability in the antenna terminations.

For testing the wireless link, the antennas need to be matched to 50  $\Omega$  instruments. To bi-conjugate match the system, we computed the unique matched source and load terminations to achieve this and implement matching circuits comprised of two reactive components for both antennas. This is a generally applicable approach to transform any complex impedance to a given resistance [10, Ch. 5.1]. In this process, we utilised the simulated Z-parameters of the wireless link including the antennas and biological channel that we obtained from simulations in ANSYS HFSS as detailed in [3]. As shown in [3], due to the miniature size of the implanted antenna and the biological environment, the maximum link power efficiency in this system is attained around 300 MHz. At this frequency, the component values to realize the bi-conjugate matching were found to be:  $C_{in} = 13.0$  pF,  $L_{in} = 1.80$  nH,  $C_{out} = 182$  pF, and  $L_{out} = 0.75$  nH, where the capacitors are connected in series with the external and implant antennas and followed by the inductors in parallel. At 300 MHz these circuits transform 50  $\Omega$  to the matched source and load impedances  $Z_{ms} = 0.695 - j63.616 \Omega$  and  $Z_{mL} = 0.049 - j2.489 \Omega$  terminating the implant and external antenna ports, respectively. This means that under ideal conditions the system is bi-conjugate matched at 300 MHz with no impedance mismatch loss. For the assessment of impact of variability in the antenna terminations, the bounds of impedance variation can be defined in numerous ways. We first considered the tolerance rectangles  $U_S$  and  $U_L$  to be the largest squares centred at  $Z_{ms}$  and  $Z_{mL}$ , such that the minimum of  $G_T$  at 300 MHz was 3 dB (Case 1a) and 6 dB (Case 2a) below

Table 1: Percentage variation in the source and load impedance for the computation of the minimum and maximum of  $G_T$  and  $A_V$  in Fig. 4

Case 1a			
Re( $Z_S$ )	Im( $Z_S$ )	Re( $Z_L$ )	Im( $Z_L$ )
$\pm 1.17\%$	$\pm 1.17\%$	$\pm 1.17\%$	$\pm 1.17\%$
Case 1b			
Re( $Z_S$ )	Im( $Z_S$ )	Re( $Z_L$ )	Im( $Z_L$ )
-1.17%	$\pm 1.17\%$	-1.29%	-1.21%
+364%		+21.1%	+1.18%
Case 2a			
Re( $Z_S$ )	Im( $Z_S$ )	Re( $Z_L$ )	Im( $Z_L$ )
$\pm 1.94\%$	$\pm 1.94\%$	$\pm 1.94\%$	$\pm 1.94\%$
Case 2b			
Re( $Z_S$ )	Im( $Z_S$ )	Re( $Z_L$ )	Im( $Z_L$ )
-2.24%	$\pm 1.94\%$	-1.96%	-1.95%
+1013%		+55.1%	+1.94%

Table 2: Corner points of the tolerance rectangles (unit:  $\Omega$ ) at 300 MHz for the computation of the minimum and maximum of  $G_T$  and  $A_V$  in Fig. 4

Case 1a				
	0.228	0.228	0.233	0.233
$U_S$	$-j37.72$	$-j36.85$	$-j37.72$	$-j36.85$
$U_L$	0.039	0.039	0.0404	0.0404
	$-j1.517$	$-j1.482$	$-j1.517$	$-j1.482$
Case 1b				
	0.228	0.228	1.07	1.07
$U_S$	$-j37.72$	$-j36.85$	$-j36.85$	$-j36.13$
$U_L$	0.039	0.039	0.0483	0.0483
	$-j1.518$	$-j1.482$	$-j1.518$	$-j1.482$
Case 2a				
	0.226	0.226	0.235	0.235
$U_S$	$-j38.0$	$-j36.56$	$-j38.0$	$-j36.56$
$U_L$	0.0391	0.0391	0.0407	0.0407
	$-j1.529$	$-j1.471$	$-j1.529$	$-j1.471$
Case 2b				
	0.225	0.225	2.564	2.564
$U_S$	$-j38.0$	$-j36.56$	$-j38.0$	$-j36.56$
$U_L$	0.0391	0.0391	0.0619	0.0619
	$-j1.529$	$-j1.471$	$-j1.529$	$-j1.471$

the nominal value. As the presented analysis method is applicable to any rectangle, we then extended the squares to largest rectangles so that the drop in  $G_T$  from the nominal value remained at 3 dB (Case 1b) and 6 dB (Case 2b) at 300 MHz. Given that the level sets of

$G_T$  are circles with the properties detailed in Section II, this can be understood as an extension of the rectangles until the critical level set circle passes through not only one, but at least two of the corners of the

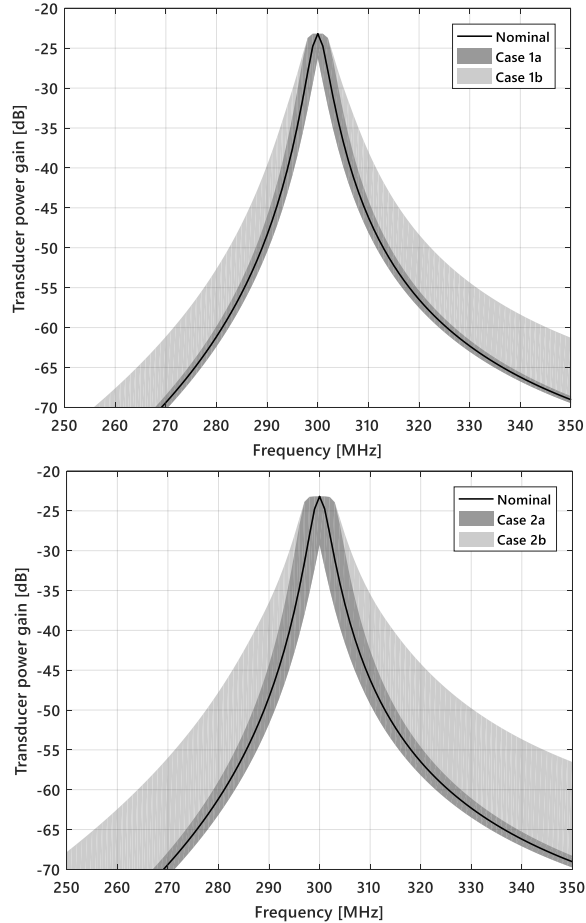


Fig. 4. Transducer power gain of the biotelemetry system and the bounds of variation as the source and load impedances vary in the tolerance rectangles given in Table 1.

tolerance rectangles. Finally, at other frequencies,  $U_S$  and  $U_L$  were defined through corner points having the same percentage difference in real and imaginary parts with respect to  $Z_S$  and  $Z_L$ , as in the case at 300 MHz. Table 1 lists the percentage differences defining the rectangles. Table 2 shows the corner points of the rectangles at 300 MHz. Figures 4 and 5 present the simulated transducer power gain and voltage gain of the system together with the bounds of variation given by the impedance tolerance defined in Table 1.

As seen from Tables 1 and 2, the bounds of variability which correspond to the notable reductions of 3 dB (Case 1) and 6 dB in the transducer power gain compared to the nominal operating conditions, are small. The same conclusion applies to voltage gain, which drops 1.6 dB and 5.3 dB in Case 1a and Case 1b, respectively, and 3.1 dB and 9.3 dB in Case 2a and Case 2b, respectively, at 300 MHz. Overall, it is clear from the results that in this system very small variations in the

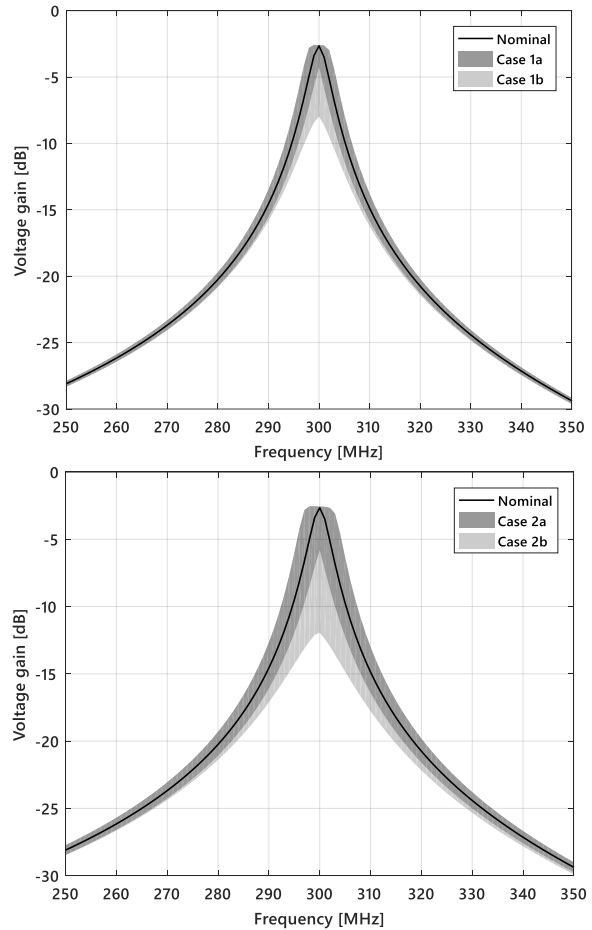


Fig. 5. Voltage gain of the biotelemetry system and the bounds of variation as the source and load impedances vary in the tolerance rectangles given in Table 1

order of 1-to-2 % in the antenna terminations may result in significant reduction in the system's performance. In contrast, however, it tolerates marked deviations in the source and load resistances, towards values higher than the nominal as exemplified by Cases 1b and 2b.

## VI. CONCLUSION

Prediction of the performance bounds of electromagnetic systems under non-ideal operating conditions is an important step in achieving reliable devices and conducting reproducible experiments. To aid this process in the context of two-port networks, we developed a semi-analytical method for locating the minimiser and maximiser of the transducer power gain and voltage gain as the port terminations vary in bounded rectangles in the complex plane. Instead of differentiation, the method exploits the knowledge on the structure of the level sets of the gain parameters to limit the numerical search to small-dimensional subsets of the full four-dimension search space. We applied the method

in the analysis of a highly sensitive biotelemetry system based on magnetically coupled small loops. Future work includes comparison of matching circuits to reduce the sensitivity in this type of wireless systems.

### ACKNOWLEDGMENT

This research was funded by Academy of Finland funding decision 294616.

### REFERENCES

- [1] J. Kimionis, M. Isakov, B. S. Koh, A. Georgiadis, M. M. Tentzeris, "3D-printed origami packaging with inkjet-printed antennas for RF harvesting sensors," *IEEE Trans. Microw. Theory Techn.*, vol. 63, no. 12, pp. 4521-4532, Dec. 2015.
- [2] M. Zargham, P. G. Gulak, "Fully integrated on-chip coil in 0.13  $\mu\text{m}$  CMOS for wireless power transfer through biological media," *IEEE Trans. Biomed. Circuits Syst.*, vol. 9, no. 2, pp. 259-271, Apr. 2015.
- [3] E. Moradi, S. Amendola, T. Björninen, L. Sydänheimo, J. M. Carmena, J. M. Rabaey, L. Ukkonen, "Backscattering neural tags for wireless brain-machine interface system," *IEEE Trans. Antennas. Propag.*, vol. 62, no. 2, pp. 719-726, Dec. 2014.
- [4] M. Waqas A. Khan, T. Björninen, L. Sydänheimo, L. Ukkonen, "Characterization of two-turns external loop antenna with magnetic core for efficient wireless powering of cortical implants," *IEEE Antennas Wireless Propag. Lett.*, vol. 15, pp. 1410-1413, Dec. 2015.
- [5] G. I. Vasilescu, T. Redon, "A new approach to sensitivity computation of microwave circuits," *IEEE Intl. Symp. Circuits and Systems*, Espoo, Finland, pp. 1167-1170, June 1988.
- [6] F. Güneş, S. Altunç "Gain-sensitivity analysis for cascaded two-ports and application to distributed-parameter amplifiers," *Intl. J. RF and Microw. Computer-Aided Eng.*, vol. 14, no. 5, pp. 462-474, Sep. 2004.
- [7] W. Ciccognani, P. E. Longhi, S. Colangeli, E. Limiti, "Constant mismatch circles and application to low-noise microwave amplifier design," *IEEE Trans. Microw. Theory Techn.*, vol. 61, no. 12, pp. 4154-4167, Dec. 2013.
- [8] P. Marietti, G. Scotti, A. Trifiletti, G. Viviani, "Stability criterion for two-port network with input and output terminations varying in elliptic regions," *IEEE Trans. Microw. Theory Techn.*, vol. 54, no. 12, pp. 4049-4055, Dec. 2006.
- [9] Ralph S. Carson, *High-Frequency Amplifiers*, John Wiley & Sons, USA, 1975.
- [10] Patrick M. Fitzpatrick, *Advanced Calculus*, 2<sup>nd</sup> ed., Thomson Brooks/Cole, USA, 2006.

- [11] David M. Pozar, *Microwave Engineering*, 4<sup>th</sup> ed., John Wiley & Sons, Inc., USA, 2012.
- [12] T. Björninen, E. Moradi, M. Waqas A. Khan, Leena Ukkonen, "Minimum of two-port voltage and power gain under varying terminations: semi-analytic method and application to biotelemetry systems," *URSI Commission B Intl. Symp. On Electromagnetic Theory*, Espoo, Finland, pp. 869-872, Aug. 2016.



**Toni Björninen** received the M.Sc. and doctoral degrees in Electrical Engineering in 2009 and 2012, respectively, from Tampere University of Technology (TUT), Tampere, Finland. He is currently an Academy of Finland Research Fellow in BioMediTech Institute and Faculty of Biomedical Sciences and Engineering in TUT. He has been a Visiting Postdoctoral Scholar in Berkeley Wireless Research Center in UC Berkeley and in Microwave and Antenna Institute in Electronic Engineering Dept., Tsinghua University, Beijing. His research focuses on technology for wireless health including implantable and wearable antennas and sensors, and RFID-inspired wireless solutions. Dr. Björninen is an author of 140 peer-reviewed scientific publications. He serves as an Associate Editor in IET Electronics Letters and IEEE Journal of Radio Frequency Identification, and as an Editor in International Journal of Antennas and Propagation. In 2016, IEEE Antennas and Propagation Society selected him among the top 10 reviewers of IEEE Transactions on Antennas and Propagation for his input during 06/2015–04/2016.